Journal of Non-Crystalline Solids 359 (2013) 56–59

Contents lists available at SciVerse ScienceDirect

Journal of Non-Crystalline Solids

journal homepage: www.elsevier.com/ locate/ jnoncrysol

Thermal characterization of glasses prepared from simulated compositions of lunar soil JSC-1A

A.S. Pinheiro [a], Z.M. da Costa [a], M.J.V. Bell [a,*], V. Anjos [a], S.T. Reis [b], C.S. Ray [b]

[a] Departamento de Física, Universidade Federal de Juiz de Fora, Juiz de Fora, MG, 36036-330, Brazil
[b] Missouri University of Science and Technology, 1870 Miner Circle, Rolla, MO 65409, USA

ARTICLE INFO

Article history:
Received 29 June 2012
Received in revised form 13 September 2012
Available online 7 November 2012

Keywords:
JSC-1A;
Lunar simulant;
Glasses;
Thermal diffusivity;
Photoacoustics

ABSTRACT

The thermal conductivity (K), thermal diffusivity (α), and specific heat capacity (ρc) for a glass prepared from JSC-1A lunar soil simulant were measured using a combination of open photoacoustic cell (OPC) and thermal relaxation techniques. The values of K and α for the JSC-1A glass were (20 ± 3) mW/cmK and (14 ± 2) cm^2/s, respectively, and are somewhat larger than those of the comparable silicate glasses. The specific heat capacity (ρc) for this glass was (1.44 ± 0.07) J/cm^{3}K, which is a little smaller than the comparable silicate glasses. Materials with high values of K and α rapidly adjust their temperature with that of their surrounding atmosphere, making them more resistant to mechanical failure occurring due to thermal shock.

1. Introduction

The National Aeronautics and Space Administration (NASA) approved and released a simulated composition of lunar regolith, called JSC-1, to conduct research and develop technologies to support the needs for a future human habitat on the surface of the Moon, and to advance its space exploration program [1–4]. The JSC-1 lunar simulant was prepared from the volcanic ash eruptions from vents on the south side of Merriam Crater in San Francisco volcanic field, north of Flagstaff, Arizona, USA [5]. Supply of this simulant has been exhausted eventually and NASA released a lunar Maria simulant material, commonly known as JSC-1A, to the research community to support studies related to lunar surface operation. The JSC-1A simulant is from the same quarry as JSC-1 and has a chemical composition close to that of the JSC-1. The overall composition of JSC-1 or JSC-1A [5] is also close to that of the lunar soil samples collected by the Apollo 14 [6,7] and Apollo 17 [8] missions (see Table 1). The studies described herein are for a glass prepared from the JSC-1A lunar soil simulant.

The most abundant material in the lunar soil, and so in JSC-1 or JSC-1A, is SiO_2 which is the primary ingredient for manufacturing most of the commercial glass and glass ceramic products. Thus, there is a high possibility that glasses can be prepared also from the lunar soil. Since glass and glass-derived products are one of the most used materials by mankind, any future habitat on the Moon may also find the use of these materials essential. Therefore, it is important to know what kind of glasses can be developed from the lunar soil and what kind of application potentials they might have.

The glass formation tendency of melts from the JSC-1 and JSC-1A lunar soil simulants and characterization of the glasses prepared from these simulants using X-ray diffraction analysis (XRD), differential thermal and thermo-gravimetric analysis (DTA/TGA), scanning electron microscopy (SEM), chemical analysis for composition by inductively coupled plasma atomic absorption spectroscopy (ICP-AES), EPR and Mössbauer spectroscopy have been reported previously [9,10]. The present work which is an extension of the previous work [9,10], reports measurements of selected important properties, namely, thermal diffusivity (α), thermal conductivity (K), and heat capacity (C) for the glass prepared from JSC-1A lunar soil simulant, so as to make the property data base for this important glass broader and comprehensive. These properties are important to understanding the response and behavior of materials that undergo adverse thermal cycling, such as what is experienced by the surface of the Moon. A high thermal conductivity assures a uniform temperature distribution in the material, which reduces thermally induced stresses and, hence, improves fatigue properties. The thermal diffusivity measures the rate at which heat is conducted or dissipated in a material.

Among the commonly used techniques to obtain α, Photoacoustic (PA) has been widely used due to its high sensitivity. The thermal conductivity was obtained by volumetric heat capacity measurements which allow determining the product ρc, where ρ is the density and c the specific heat. To our knowledge this is the first time photoacoustics and ρc have been used to determine the thermal diffusivity, thermal conductivity and specific heat of JSC-1A lunar soil simulant.

* Corresponding author. Tel.: +55 3221023307; fax: +55 3221023312.
E-mail address: mjbell@fisica.ufjf.br (M.J.V. Bell).

0022-3093/$ – see front matter © 2012 Elsevier B.V. All rights reserved.
http://dx.doi.org/10.1016/j.jnoncrysol.2012.09.027

Table 1
Composition (wt.%) of the JSC-1 and JSC-1A lunar soil simulants, and of the soil samples collected from the Moon's surface by Apollo 14 and Apollo 17 missions.

Oxide components	SiO_2	Al_2O_3	TiO_2	Fe_2O_3	MnO	CaO	MgO	K_2O	Na_2O	P_2O_5	FeO
JSC-1A	45.7	16.2	1.9	12.4	8.7	10.0	8.7	0.8	3.2	0.7	-
JSC-1	47.7	15.0	1.6	3.4	0.2	10.4	9.0	0.8	2.7	0.7	7.4
Appolo 14	47.3	17.8	1.6	0.0	0.1	11.4	9.6	0.6	0.7	0.0	10.5
Appolo 17	42.2	15.7	5.1	0.0	0.2	11.5	10.3	0.1	0.2	0.0	12.4

2. Experimental setup

The glasses from the JSC-1A soil simulant were prepared by melting the simulant between 1500 and 1550 °C in platinum crucibles in air for about 3 h. A typical melt size was approximately 50 g. Melts were quenched on steel plates and glasses were annealed for 6 h near the respective glass transition temperature, ~695 °C. The thicknesses of the samples were (230 ± 2) μm and (500 ± 2) μm for PA and heat capacity measurements, respectively.

The Photoacoustic experiment was performed using a Hg–Xe lamp (500 W). The outgoing light was modulated by a chopper (SR 540) and an open PA cell was used. Basically this cell consists of gluing with vacuum grease a solid sample directly above a circular commercial piezoelectric microphone (see inset Fig. 1). The front chamber of the microphone itself acts as the usual gas chamber of conventional photoacoustics and is a minimal-volume photoacoustic system of detection. Such a minimal volume corresponds to the volume of the camera of the microphone only, which is the minimum possible volume. The use of a minimal gas chamber considerably increases the signal-to-noise ratio and requires minimal experimental arrangements. Periodic heating of the sample by absorption of the modulated light, produces a periodic oscillation of pressure in the chamber, causing deflections on the diaphragm of the microphone, generating a voltage across a resistor. The signal is amplified by a lock-in SRS 530 which records the amplitude and phase of the signal as a function of the chopper frequency.

Heat capacity measurements were performed according to the procedures described in reference [11]. The bulk sample of glass was polished and sprayed with black paint on both sides of their larger surfaces. The sample while adiabatically suspended in a vacuum sealed Dewar flask, was heated with an Argon laser tuned at 514 nm and 35 mW. The laser light passes through the Dewar by means of a transparent window. A heating curve is recorded as a function of time via a thermocouple attached to the opposite surfaces of the sample. Thermal paste was used to improve the thermal contact. After this procedure the laser is blocked and a cooling curve is obtained. In order to obtain better experimental results concerning heat capacity measurements the sample was thinned to 500 μm thick as the lateral dimensions of it were neglected in the calculations.

The experimental results were fitted with the theoretical equations of the suitable model via Origin®. The errors of the thermal diffusivity, thermal conductivity and of the specific heat capacity where calculated from the error of the Origin® propagated jointly with the error of the samples thickness.

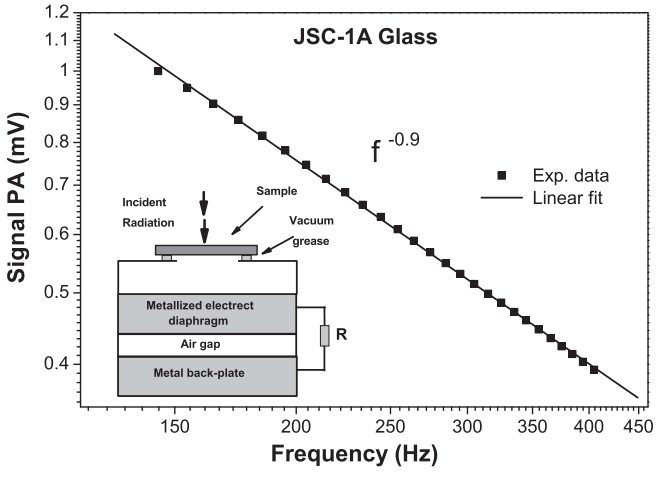

Fig. 1. Microphone output voltage (PA signal) as a function of the modulation frequency for a (230 ± 2) μm thick glass prepared from JSC-1A lunar soil simulant. The solid curve shows approximately a $f^{-1,0}$ dependence ($f^{-0,9}$). Inset: schematic diagram of an open photoacoustic cell.

3. Theory

Photoacoustics is a photothermal technique where modulated light impinges the sample held in a photoacoustic cell. A fraction of the incident energy is absorbed by the sample, and the heat generated due to the non-radiative relaxation causes the temperature of the sample to increase. The heat diffuses into the air (chamber A) adjacent to the sample causing its temperature to increase. For a cell with a fixed volume this produces a corresponding increase in pressure which is detected by the microphone (pressure fluctuations are converted into electric current). Several models and experimental setups have been developed to obtain the thermal diffusivity of the sample from the measured acoustic waves. Concerning the theory of Open Photoacoustic Cell (OPC) three processes that are dependent upon the characteristics of the material may be found:

(1) ***Thermal diffusion*** (Rosencwaig and Gersho or RG model) [12]. The heat generated by absorption of light is diffused through the sample by heating a thin layer of air in contact with the opposite surface of the sample. This thin layer is defined as one comparable to the diffusion length of air [12]. It generates a pressure wave that results in the photoacoustic signal. This model considers this thin layer of air as an acoustic piston to generate the photoacoustic signal and is called the acoustic piston model of Rosencwaig and Gersho [12]. For the regime of (thermally thick) sample, the photoacoustic signal decreases exponentially with the frequency modulation, given by Eq. (1):

$$S = \frac{A}{f} e^{-a\sqrt{f}} \tag{1}$$

where $a = l_s \sqrt{\pi/\alpha}$, l_s is the sample thickness and α is the thermal diffusivity. A thermally thick or thin sample is defined according to Ref. [12], where the sample thickness is compared with the thermal diffusion length of the material. The constant A includes all residual factors such as the (gas thermal properties). In this case, the phase ϕ depends on the modulation frequency f by the relation:

$$\phi = -\frac{\pi}{2} - a\sqrt{f}. \tag{2}$$

This RG process is generally valid in the low frequency range, preferably for f where $(f/f_c)^{1/2} < 0.4$ [13]. Here f_c is the frequency where the sample thickness is equal to the length of thermal diffusion.

(2) ***Thermo-elastic bending*** [12]. It may be applied in the case of plate-shaped solid samples surrounded by air. Basically this contribution takes into account the bending of the sample

due to the existence of a temperature gradient inside it and along the direction of light incidence (z-axis). As a result, a z-dependent thermal expansion occurs which produces a strain perpendicular to the z-axis, and causes the sample to bend. The result is a vibrating sample acting as a drum, thereby contributing to the PA signal. In this case [12], the PA signal presents, in the thermally thick region, a f^{-1} frequency dependence as well as a phase that tends to $\pi/2$ whose expression is given by:

$$\phi_{el} \approx \frac{\pi}{2} + \arctan\left[{}^{1}\!/_{a}\sqrt{f} - 1\right] \tag{3}$$

(3) ***Thermal dilatation***. In this mechanism the PA signal also presents a $f^{-1.0}$ dependence in the thermally thick region [16]. However, the photoacoustic phase is independent of the modulation frequency. This mechanism is hardly seen in the OPC configuration. The reason is that the previous models (RG and thermo-elastic bending) give much higher photoacoustic signal than the thermal dilatation model [13].

The appropriate mechanism that is applicable to a specific material is determined by observing the photoacoustic signal and phase in OPC measurements as a function of the modulation frequency.

In order to obtain the heat capacity of solids, the thermal relaxation method is used. It relies in the record of the thermal heating or thermal relaxation of the sample as a function of time in the presence or absence of illumination. The heat capacity is related to the time the sample takes to heat or to cool through the relation [11]:

$$\Delta T = T_f - T_0 = \left(\frac{T_f^4 - T_0^4}{4T_0^3}\right)\left[1 - \exp\left({}^{t}\!/_{\tau_r}\right)\right], \tag{4}$$

where two considerations are used: a) only radiation losses are taken into account and (b) the temperature changes induced by the illumination are small compared to the surrounding environment temperature. In Eq. (4), T_f is the temperature when the sample reaches the equilibrium, T_0 is the initial temperature of the sample, $\tau_r = \rho c l_s / 8\sigma T_0^3$ where ρc is the specific heat capacity, and σ is the Stefan–Boltzmann constant.

4. Results

Fig. 1 shows the log-log plot of the PA signal for a (230 ± 2) μm thick glass prepared from JSC-1A lunar soil simulant as a function of the modulation frequency between 150 and 400 Hz. From this figure, in the frequency range of 150 to 400 Hz the sample is in the thermally thick regime, where the thickness of the sample is larger than the thermal diffusion length of the sample [12]. It presents a $f^{-0,9}$ dependence which suggest a thermal bending mechanism or thermal dilatation mechanism. In order to identify the exact controlling mechanism we investigated the PA phase. This is shown in Fig. 2. The fitting of this curve is in agreement with what can be expected for the thermoelastic model; for the thermal dilatation model the phase should be constant which is not the case. Once the underlying photoacoustic mechanism is identified to be thermoelastic, the value of "a" can be determined using Eq. (3) and that of α (thermal diffusivity) can be calculated using the relation, $a = l_s\sqrt{{}^{\pi}\!/_{\alpha}}$ which is (0.014 ± 0.002) cm^2/s for the JSC-1A glass.

The thermal relaxation data of the glass ((500 ± 2) μm thick) obtained as a function of time for the specific heat capacity measurement are shown in Fig. 3. The data points, when fitted using Eq. (4), (solid line in Fig. 3) yield a value of ρc as (1.44 ± 0.07) J/cm^{3}K. The thermal conductivity, K, was then calculated using the expression, $K = \alpha\rho c$, which is (0.020 ± 0.003) W/cmK for the JSC-1A glass. For comparison, the values of thermal conductivity, thermal diffusivity and ρc obtained from the present measurements for the JSC-1A glass have been shown in Table 2 along with those for some standard silicate glasses [14,15].

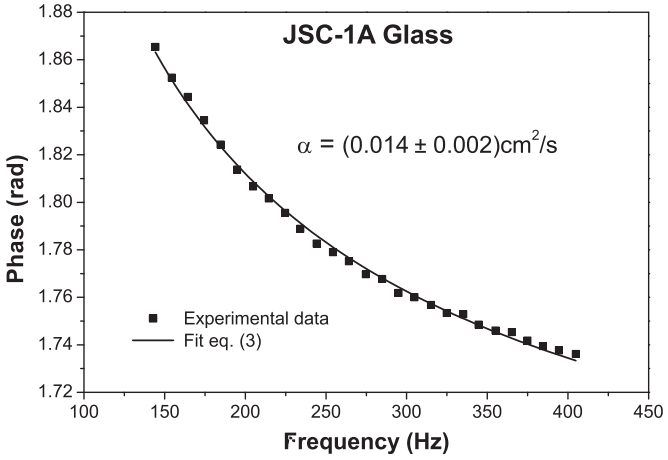

Fig. 2. Phase of the PA signal as a function of modulation frequency for the JSC-1A lunar soil simulant glass.

5. Discussion

The heat propagation in disordered materials is usually understood in terms of the Debye model, where the thermal conductivity is proportional to:

$$K \propto cvl \tag{7}$$

where c is the volumetric heat capacity, v is the average phonon velocity and l, the mean free path of phonons. If the lattice interactions were harmonic, one should expect very high values for the mean free path, and consequently, high thermal conductivities. Nevertheless, small values of l result from anharmonic terms, that limit the mean free path by coupling together the various lattice vibrations. Moreover, the mean free path is usually limited by geometrical effects associated with the disordered nature of glasses. In other words, the thermal properties of glass are interpreted in terms of an approximately constant mean free path for lattice phonons, usually of the order of magnitude of the scale of structural disorder at the atomic or molecular level. As a consequence, the thermal conductivity is dominated by the heat capacity and phonon velocity and it is normally lower than the respective crystalline form of the glass components.

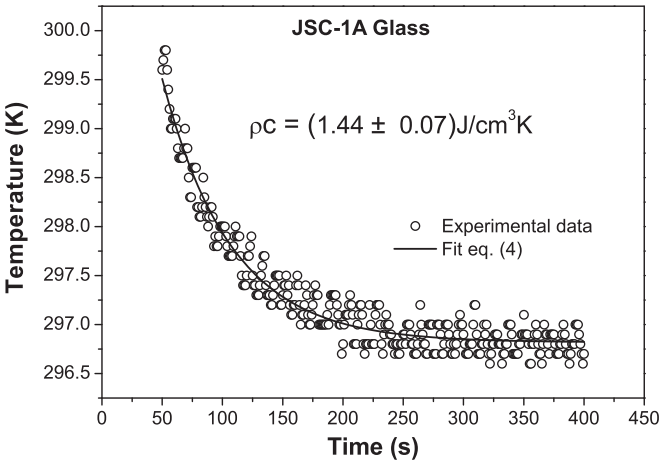

Fig. 3. Cooling curve of the specific heat capacity measurements for a (500 ± 2) μm thick JSC-1A lunar soil simulant glass as a function of time.

Table 2
Thermal properties of the glass prepared from JSC-1A lunar soil simulant compared to some standard silicate glasses.

Glass composition (mol%)	ρc (J/cm^3K)	α (10^{-3} cm^2/s)	K (mW/cmK)	Ref.
JSC-1A	1.44 ± 0.07	14 ± 2	20 ± 3	This work
$39SiO_2$–$25Al_2O_3$–31.4CaO–4.1MgO	2.30 ± 0.06	4.9 ± 0.2	11.2 ± 0.8	[14]
$74SiO_2$–$13Na_2O$–10.5CaO–$1.3Al_2O_3$–$0.3K_2O$,–$0.2SO_3$–0.2MgO–$0.04Fe_2O_3$–$0.01TiO_2$	2.04	Not reported	9 to 13	[15]

Also it is known that the thermal diffusivity α is very sensitive to changes in network topology of disordered materials, such as glasses.

It has been assumed that the thermal conductivity of a glass decreases when the composition of the glass is more complex, due to the shortening of phonon mean free path that results from the increasing disorder of the glass structure. To understand and interpret the effect on the thermal conductivity by adding monovalent or divalent oxides, the effect of such oxides on the geometrical arrangement of the building units of the glassy network need to be considered. In this sense we can observe that the JSC-1A is a complex glass that leads to the conclusion it should have low thermal conductivity. However, the presence of Fe_2O_3 that is a very efficient thermal conductor makes the JSC-1A glass a good thermal conductor when compared with other complex glasses. According to reference [17], the thermal conductivity of Fe_2O_3 is 150 mW/cmK. Similar results were also found for iron phosphate glasses, with elevated fraction of Fe_2O_3 [18].

6. Conclusion

The thermal diffusivity, thermal conductivity, and specific heat capacity of a glass prepared from the JSC-1A lunar soil simulant were measured by open photoacoustic cell and thermal relaxation techniques. The glass from the JSC-1A soil simulant is characterized to have a high thermal conductivity when compared with other glasses with similar composition. The effect is attributed to the presence of Fe_2O_3 in the JSC-1A composition. Substances with high thermal diffusivity rapidly adjust their temperature to that of their surroundings, because they conduct heat quickly in comparison to their volumetric heat capacity. The simulated lunar glass therefore may be a suitable material for use in the construction of habitats and landing surfaces for space vehicles since, from thermal point of view, it could respond well to large temperature variation that occurs on the Moon.

Acknowledgments

Authors want to thank the Brazilian agencies CAPES, CNPq and FAPEMIG for financial support.

References

[1] E.C. Aldridge, Report on the President's Commission on Implementation of United States Space Exploration Policy. Available at: http://www.nasa.gov/pdf/60736main_M2M_report_small.pdf June 2004.
[2] P.A. Curreri, E.C. Ethridge, S.B. Hudson, T.Y. Miller, R.N. Grugel, S. Sen, D.R. Sadoway, Process Demonstration for Lunar In Situ Resource Utilization—Molten Oxide Electrolysis, NASA Technical Report 214600, August 2006. Available at: http://isru.msfc.nasa.gov/lib/Documents/PDF%20Files/NASA_TM_06_214600.pdf.
[3] A. Freundlich, T. Kubricht, A. Ignatiev, in: AIP Conference Proceeding of the Space Technology and Applications International Forum, v. 420, January 1998, pp. 660–665.
[4] J. Wilson, W. Towsend, L.W. Towsend, W. Schimmerling, G.S. Khandelwal, F. Khan, J.E. Nealy, F.A. Cucinotta, L.C. Simonsen, J.L. Shinn, J.W. Norbury, J.W. Norbury, Transport methods and interactions for space radiation. Chapter 12 in: NASA Langley Technical Report, 2003, pp. 500–503.
[5] J.J. Papike, S.B. Simon, J.C. Laul, Rev. Geophys. Space Phys. 20 (1982) 761–826.
[6] G. Heiken, D. Vaniman, B.M. French, in: Lunar Source Book—A Use Guide to the Moon, second ed., Lunar and Planetary Institute, Cambridge University Press, 1993, p. 27.
[7] P. Eckart, The Lunar Base Handbook, The McGraw Hill, 1999.
[8] E. Hill, M.J. Mellin, B. Deane, Y. Liu, L.A. Taylor, Appolo sample 70051 and high- and low-Ti lunar soil simulants MLS-1A and JSC-1A: Implications for future lunar exploration, J. Geophys. Res. Planets 112 (2007);
a J.L. Klosky, S. Sture, H.Y. Ko, F. Barnes, ASCE J. Aerospace Eng. 13 (2000) 133–138.
[9] C.S. Ray, S.T. Reis, W.M. Pontuschka, J.B. Yang, F.F. Sene, J.M. Giehl, C.W. Kim, S. Sen, J. Non-Cryst. Solids 352 (2006) 3677–3684.
[10] C.S. Ray, S.T. Reis, S. Sen, J.S. O'Dell, J. Non-Cryst. Solids 356 (2010) 2369–2374.
[11] V. Anjos, M.J.V. Bell, E.A. de Vasconcelos, E.F. da Silva, A.A. Andrade, R.W.A. Franco, M.P.P. Castro, I.A. Esquef, R.T. Faria, Microelectron. J. 36 (2005) 977–980.
[12] A. Rosencwaig, Gersho, J. Appl. Phys. 47 (1976) 64–69.
[13] G. Rousset, F. Lepoutre, L. Bertrand, J. Appl. Phys. 54 (1983) 2383–2391.
[14] A. Steimacher, N.G.C. Astrath, A. Novatski, F. Pedrochi, A.C. Bento, M.L. Baesso, A.N. Medina, J. Non-Cryst. Solids 352 (2006) 3613–3617.
[15] L.P.B.M. Janssen, M.M.C.G. Warmoeskerken, Transport Phenomena Data Companion, VVSD, Delft, 2006.
[16] L.F. Perondi, L.C.M. Miranda, J. Appl. Phys. 62 (1987) 2955.
[17] M. Takeda, T. Onishi, S. Nakakubo, S. Fujimoto, Mater. Trans. 50 (2009) 2242–2246.
[18] A.P. Silva, Z.M. Costa, V. Anjos, M.J.V. Bell, S.T. Reis, N.O. Dantas, Opt. Mater. 33 (2011) 1975–1979.